Ingeniería y Ciencia
ISSN:1794-9165 | ISSN-e: 2256-4314
ing. cienc., vol. 13, no. 26, pp. 147–171, julio-diciembre. 2017.
http://www.eafit.edu.co/ingciencia

A Generalized Model and Control for Supermagnetic and Supercapacitor Energy Storage

Walter Julián Gil-González[1], Alejandro Garcés[2] and Andrés Escobar[3]

Received: 17-08-2017 | Accepted: 06-10-2017 | Online: 14-11-2017

MSC:68U20, 97C30, 97D50, 97U70

doi:10.17230/ingciencia.13.26.6

Abstract

This paper presents a generalized linear model based on LMI state-feedback with integral action, applicable to the control of Electric Energy Storage Systems (EESS) such as Superconducting Magnetic Energy Storage (SMES) and Supercapacitor Energy Storage (SCES). A Voltage Source Converter (VSC) and a Pulse-Width modulated Current Source Converter (PWM-CSC) are respectively used to integrate the SCES and the SMES systems to the electrical distribution system. To represent the dynamics between the EESS and the power distribution system a reduced general linear model in the state-space representation is introduced. The proposed control scheme regulates independently the active and reactive power flow between the EESS and ac the grid. Three case scenarios comparing a conventional PI controller and the proposed technique are conducted considering grid voltage fluctuations. Extensive time-domain simulations demonstrate the robustness and proper performance of the proposed controller to

[1] Universidad Tecnológica de Pereira, wjgil@utp.edu.co,
http://orcid.org/0000-0001-7609-1197, Pereira, Colombia.
[2] Universidad Tecnológica de Pereira, alejandro.garces@utp.edu.co, Pereira, Colombia.
[3] Universidad Tecnológica de Pereira, andreses1@utp.edu.co, Pereira, Colombia.

operate the EESS as power compensator, in order to improve the operative conditions of electrical distribution systems.

Key words: Electric energy storage systems (EESS); linear matrix inequality (LMI); supercapacitor energy storage (SCES); superconducting magnetic energy storage (SMES).

Un modelo generalizado y controlpara almacenadores de energía por superconductor magnético y supercondesador

Resumen

En este articulo se presenta un control de retroalimentación a un modelo lineal generalizado basados en LMI con seguimiento de acción integral para sistemas de almacenamiento de energía eléctrica (SESS) tales como: a almacenamiento de energía magnética por superconducción (SMES) y almacenamiento de energía eléctrica por supercondensador (SCES). Un compacto de modelo lineal general en la representación del espacio de estado para representar el comportamiento dinámico entre el SESS y el sistema de distribución es presentado. Para integrar los sistemas SCES y SMES al sistema de distribución se utilizan un convertidor de fuente de tensión (VSC) y un convertidor de fuente de corriente modulada por ancho de pulso (PWM-CSC), respectivamente. La estrategia de control propuesta permite el control bidireccional de la potencia activa y reactiva entre el EESS y la red *ac* de manera independiente. Los resultados de las simulaciones demuestran el desempeño robusto y eficiente del control propuesto para operar EESS como compensadores de potencia activa y reactiva, con el fin de mejorar las condiciones operativas en el sistema de distribución. Además, todos los casos propuestos se compararon con el controlador PI convencional para verificar su validez.

Palabras clave: Sistemas de almacenamiento de energía eléctrica (SESS); desigualdades matriciales lineales (LMI); almacenamiento de energía supercondensador (SCES); almacenamiento de energía magnética superconductora (SMES).

1 Introduction

Energy storage systems (ESS) play an important role in balancing supply and demand in the electric grid. They help the power transmission and distribution systems to improve operative conditions such as power system stabilization [1], [2], load frequency control [3], [4], damping of the

torsional oscillations [5], [6], voltage regulation, and to mitigate the effect of intermittency of renewables. Depending on how the energy is stored, the ESS can be classified in electrochemical energy storage (e.g., batteries and fuel cells), mechanical energy storage (e.g., flywheels, pumped hydro and compressed) and electrical energy storage systems (EESS) (e.g., Super magnetic energy storage (SMES) and super-capacitor energy storage (SCES), which store energy in the magnetic and electric field respectively).

The ESS can be applicable in electrical power systems to: Load shifting, peak shaving, frequency and voltage control, wind and solar farms voltage fluctuations, among others. Despite their multiple advantages electrochemical and mechanical energy storage have disadvantages such as: Low efficiency, life-time limited, susceptible to charge/discharge cycles, slow response, short-time periods between maintenances, etc. Due to its capacity to improve the overall dynamical performance and smooth the energy generated by the power supply, the EESS have application in power systems with high penetration of renewables [7].

To be integrated with the grid, EESS require power electronic interfaces for the energy conversion process. The SCES is interfaced to the grid through a Voltage Source Converter (VSC) due to its inherent voltage characteristic [7], while three types of power converters can be used for the SMES as shown in Figure 1, named: line commutated converters (LCC) [4], [8], a VSC with a dc-dc chopper [9], and pulse-width modulated current source converter (PWM-CSC) [8], [10], which is the most suitable for SMES due to its inherent current characteristic.

Several control strategies have been proposed for SMES and SCES: In [1] and [11], a proportional-integral controller is introduced. A fuzzy-logic approach is presented in [12] and [13], a decoupled State-Feedback is described in [14] and [15], a model predictive controller is illustrated in [16] and finally feedback linearization is presented in [9] and [17]. Although the SMES and the SCES share a similar performance, most of the controls and dynamic models are proposed independently and yet a generalized linear control strategy for SMES and SCES has not been reported in literature. A thorough search of the relevant literature yielded only one generalized approach presented in [1], which approach only considers VSC to integration device to the ac grid.

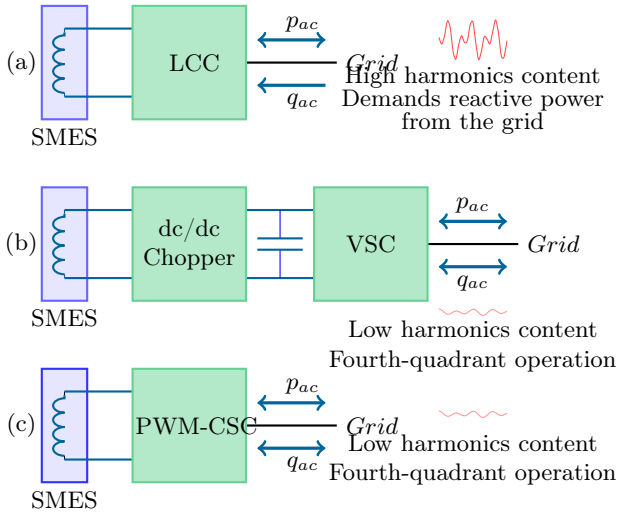

Figure 1: Three possible configurations for SMES integration: (a) LCC-Based, (b) VSC-Based, and (c) PWM-CSC-Based

The main objective of this paper it is to propose a general dynamical model to control EESS via LMI-Feedback control taking into account the properties of the VSC and PWM-CSC. To this end, a generalized linear control model using LMI-based state-feedback for EESS is presented. The proposed controller allows active and reactive power exchange between the EESS and the ac grid. Furthermore, LMI-based state-feedback is used as control technique, because it allows to find a feedback gain matrix guaranteeing stability properties in the sense of Lyapunov. It will be shown that it is not necessary to use external parametrization to define the control signal, since the control signal is directly calculated as a semi-infinite programming problem. Additionally, LMI allows to consider operating limits of the EESS, furthermore to solve the convex optimization problem CVX (a convex programming software), it is used [18].

The rest of the paper is organized as follows: Section two presents the dynamic general model of the EESS. The proposed control strategy is explained in section three. In section four it is described the test system, the simulation scenarios and the general results. Finally, section six provides conclusions and remarks of the research.

2 Dynamic general model for EESS

The dynamic general model for the EESS is obtained applying the Kirchhoff's laws at the ac side of the converter (VSC or PWM-CSC) and the Tellegen's theorem to calculate the active power transferred from the ac grid to the dc side or reversal (see Figure 2). These models are analyzed in the *dq*-frame applying Park's transformation.

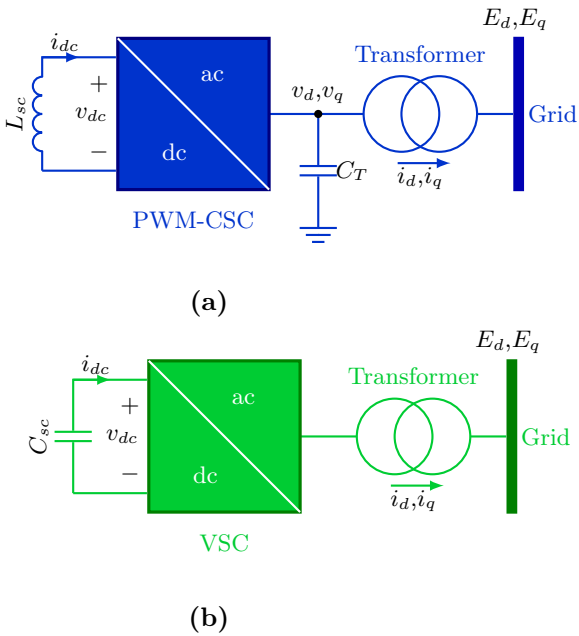

Figure 2: Connection of EESS to grid: (a) SMES (b) SCES

2.1 SMES dynamic general model

Due to the characteristics of the SMES, a power converter is required for the energy conversion process as shown in Figure 2a. Since, the SMES has a current inherent characteristic, it is more appropriate to use the PWM-CSC shown in Figure 1c. The set of equations (1) to (5) represent the dynamic general model of the SMES considering the PWM-CSC [14], [19].

$$L_T \cdot \frac{d}{dt} i_d = -R_T \cdot i_d - \omega \cdot L_T \cdot i_q + v_d - E_d \tag{1}$$

$$L_T \cdot \frac{d}{dt} i_q = -R_T \cdot i_q + \omega \cdot L_T \cdot i_d + v_q - E_q \tag{2}$$

$$C_T \cdot \frac{d}{dt} v_d = -i_d - \omega \cdot C_T \cdot v_q + m_d \cdot i_{dc} \tag{3}$$

$$C_T \cdot \frac{d}{dt} v_q = -i_q + \omega \cdot C_T \cdot v_d + m_q \cdot i_{dc} \tag{4}$$

$$\frac{1}{2} L_{sc} \cdot \frac{d}{dt} i_{dc}^2 = -\frac{3}{2} \left(E_d \cdot i_d + E_q \cdot i_q \right) \tag{5}$$

where i_d and i_q are the direct and quadrature currents of the current flowing to the coupling transformer, L_T and R_T are the inductance and resistance of the coupling transformer. ω is the frequency of the ac grid, E_d and E_q are the direct and quadrature voltages of the grid, C_T is a capacitor used as low-pass filter in the ac side of the PWM-CSC and v_d and v_q are the direct and quadrature voltages at the output of the converter. The coefficients m_d and m_q are the direct and quadrature modulation indexes respectively, which are related to the control signals limited between -1 and 1 (to avoid over-modulation of the power converter). Finally, L_{sc} corresponds to the inductance of the SMES, which dc current is i_{dc}. As shown, the terms $m_d \cdot i_{dc}$ and $m_q \cdot i_{dc}$ of (3) and (4) are non-linear; however, a linear model is defined by employing:

$$u_k = m_k \cdot i_{dc} \quad \forall k \in (d, q) \tag{6}$$

2.2 SCES dynamic general model

The SCES requires a power converter to be connected with ac grid as shown in Figure 2b. Since, the SCES has a voltage characteristic it is more appropriate to use a VSC that facilitates to storage energy in the electric field. The set of equations (7) to (9) represent the dynamic model of the SCES considering the VSC [15].

$$L_T \cdot \frac{d}{dt} i_d = -R_T \cdot i_d - \omega \cdot L_T \cdot i_q + m_d \cdot v_{dc} - E_d \tag{7}$$

$$L_T \cdot \frac{d}{dt} i_q = -R_T \cdot i_q + \omega \cdot L_T \cdot i_d + m_q \cdot v_{dc} - E_q \tag{8}$$

$$\frac{1}{2} C_{sc} \cdot \frac{d}{dt} v_{dc}^2 = -\frac{3}{2} \left(E_d \cdot i_d + E_q \cdot i_q \right) \tag{9}$$

where C_{sc} is the capacitance of the SCES, which dc voltage is v_{dc}. The rest of the parameters and variables have the same definition presented in the previous subsection. As indicated the terms $m_d \cdot v_c$ and $m_q \cdot v_{dc}$ of (7) and (8) are non-linear; nevertheless, a linear model can be defined as:

$$u_k = m_k \cdot v_{dc} \quad \forall k \in (d, q) \tag{10}$$

2.3 General model in state space

The dynamic model for the EESS in the state-space representation is shown in (11). This representation is more appropriate to introduce a convenient control strategy.

$$\begin{gathered} \dot{x} = A \cdot x + B \cdot u + B_w \cdot w \\ y = C \cdot x \end{gathered} \tag{11}$$

$$\dot{z} = -D \cdot w^T \cdot y \tag{12}$$

The parameters and variables given in (11) are listed in Table 1.

3 LMI-based controller

3.1 Classic formulation of LMI

A Lyapunov-based stability analysis of the linear system (11) is fundamental to evaluate the stability of systems. This types of systems can be controlled using a feedback gain as follows $u = K \cdot x$.

The systems presented in (11) is quadratically stable with unit-energy inputs if and only if there exist a function V and a matrix P that satisfies (13) that decreases along every nonzero trajectory of the linear system [20].

Table 1: Parameters and variables of the model

Variable	SMES	SCES
	$(x_1, x_2, x_3, x_4)^T$	$(x_1, x_2)^T$
x	$x_1 = i_d \quad x_2 = i_q$ $x_3 = v_d \quad x_4 = v_q$	$x_1 = i_d$ $x_2 = i_q$
u	$[u_d, u_q]^T$	$[u_d, u_q]^T$
z	i_{dc}^2	v_{dc}^2
w	$[E_d, E_q]^T$	$[E_d, E_q]^T$
A	$\begin{bmatrix} \frac{-R}{L_T} & -\omega & \frac{1}{L_T} & 0 \\ \omega & \frac{-R}{L_T} & 0 & \frac{1}{L_T} \\ \frac{-1}{C_T} & 0 & 0 & -\omega \\ 0 & \frac{-1}{C_T} & \omega & 0 \end{bmatrix}$	$\begin{bmatrix} \frac{-R}{L} & -\omega \\ \omega & \frac{-R}{L} \end{bmatrix}$
B	$\frac{1}{C_T} \cdot \begin{bmatrix} 0 & 0 & 1 & 0 \\ 0 & 0 & 0 & 1 \end{bmatrix}^T$	$\frac{1}{L_T} \cdot \begin{bmatrix} 1 & 0 \\ 0 & 1 \end{bmatrix}$
C	$\begin{bmatrix} 1 & 0 & 0 & 0 \\ 0 & 1 & 0 & 0 \end{bmatrix}^T$	$\begin{bmatrix} 1 & 0 \\ 0 & 1 \end{bmatrix}$
B	$\frac{-1}{C_T} \cdot \begin{bmatrix} 0 & 0 & 1 & 0 \\ 0 & 0 & 0 & 1 \end{bmatrix}^T$	$\frac{-1}{L_T} \cdot \begin{bmatrix} 1 & 0 \\ 0 & 1 \end{bmatrix}$
D	$\frac{3}{L_{sc}}$	$\frac{3}{C_{sc}}$

$$V(x) = x^T \cdot P \cdot x \leq \int_0^t w^T \cdot w \cdot d\tau \leq 1$$
$$P = P^T \succeq 0 \tag{13}$$

where ($\preceq$) stands for positive semi-definiteness. Therefore, V is a Lyapunov function with the decreasing characteristic represented by:

$$\begin{bmatrix} \mathcal{A}^T \cdot P + P^T \cdot \mathcal{A} & P^T \cdot B_w \\ B_w^T \cdot P & -I \end{bmatrix} \preceq 0$$
$$\mathcal{A} = A + B \cdot K \tag{14}$$

where,

$$Q = P^{-1} \tag{15}$$

$$S = K \cdot Q \tag{16}$$

Notice that if $P \succeq 0$ then $P^{-1} \succeq 0$. Replacing (15) and (16) into (14) it is obtained (17), which is a generalized convex inequality [20].

$$A \cdot Q + Q \cdot A^T + B \cdot S + S^T \cdot B^T + B_w \cdot B_w^T \preceq 0 \tag{17}$$

Hence, a basic feedback controller is achieve by solving the convex optimization problem given by:

$$\begin{array}{c} minimize \quad f(Q,Y) \\ subject\ to \quad Q \succeq 0 \\ A \cdot Q + Q \cdot A^T + B \cdot S + S^T \cdot B^T + B_w \cdot B_w^T \preceq 0 \end{array} \tag{18}$$

where f can be chosen according to any desired convex performance index. In this case, it is only relevant the feasibility of the problem in order to guarantee stability. So there is not a particular function to be minimized.

3.2 Tracking with integral action

Due to the fact that the general model of the EESS have disturbances, it is necessary to add an integral action in order to bring the steady-state error to zero. The control strategy with integral action is a good alternative to reduce this error. The main idea is to introduce an additional state in the controller that computes the integral of the error signal, which is then used as a feedback term. The integral of the tracking error is defined as [21]:

$$e = \int (r - y) \cdot dt = \int (r - C \cdot x) \cdot dt \tag{19}$$

where e is the integral of the output error which is considered as an additional state and $r = \left[x_1^{ref} x_2^{ref}\right]^T$ is the desired reference value. The variable

e is considered as an additional state and this generate a new augmented state space model combined with the set of (11) as follows:

$$\dot{\widehat{x}} = \widehat{A} \cdot \widehat{x} + \widehat{B} \cdot u + \widehat{B}_w \cdot w + \widehat{B}_r \cdot r \tag{20}$$

where,

$$\begin{array}{ll} \widehat{A} = \begin{bmatrix} A & 0 \\ -\bar{C} & 0 \end{bmatrix} & \widehat{B} = \begin{bmatrix} B \\ 0 \end{bmatrix} \quad \widehat{B}_w = \begin{bmatrix} B_w \\ 0 \end{bmatrix} \\ \widehat{B}_r = \begin{bmatrix} 0 \\ I \end{bmatrix} & \widehat{x} = \begin{bmatrix} x \\ e \end{bmatrix} \end{array} \tag{21}$$

Consequently, this stationary gain is then included in the control law as follows:

$$u = K \cdot x + K_i \cdot e = \widehat{K} \cdot \widehat{x} \tag{22}$$

where K_i is the integral action gain matrix and $\widehat{K}$ is gain matrix of augmented state space model. The matrix $\widehat{K}$ is calculated as shown in Section 3.1.

3.3 Energy storage behavior

The power exchange between the ac side and the dc side of the power converter are managed by the total energy store in the EESS as defined in (12). The solution to this differential equation is given in (23), which represents the exchange of energy between the ac side and the dc side.

$$\begin{gathered} z = z_o - D \cdot \int_0^t \mathcal{P}(\tau) \cdot d\tau \\ \mathcal{P}(\tau) = w^T \cdot y(\tau) = E_d \cdot x_1(\tau) + E_q \cdot x_2(\tau) \end{gathered} \tag{23}$$

where z_0 is the initial condition (energy stored) in the EESS and it is always large or equal to zero. $\mathcal{P}(\tau)$ corresponds to the exchange of the

active power between the EESS and the ac grid (see (5) or (9)). Notice that the energy storage can be controlled with $\mathcal{P}(\tau)$ and it is possible to define three operating conditions as follows:

- If $\mathcal{P}(\tau)$ is positive, the SMES or the SCES will be charged (i_{dc} or v_{dc} increase, respectively).
- If $\mathcal{P}(\tau)$ is negative, the SMES or the SCES will be discharge (i_{dc} or v_{dc} decrease, respectively).
- If $\mathcal{P}(\tau)$ is equal to zero, the SMES or the SCES will not transfer energy from/to the ac grid. For this reason i_{dc} or v_{dc} will be constants.

On the other hand, the active and the reactive power in the grid are calculated as given in (24) using the dq reference frame theory.

$$\begin{aligned} p_{ac} &= \tfrac{3}{2} \cdot (E_d \cdot x_1 + E_q \cdot x_2) \\ q_{ac} &= \tfrac{3}{2} \cdot (E_q \cdot x_1 - E_d \cdot x_2) \end{aligned} \tag{24}$$

Solving for x_1 and x_2 and considering the references values for the active and reactive power is possible to get:

$$\begin{aligned} x_1^{ref} &= \tfrac{2}{3} \cdot \left(\tfrac{1}{E_d^2+E_q^2}\right) \cdot \left(E_d \cdot p_{ac}^{ref} + E_q \cdot q_{ac}^{ref}\right) \\ x_2^{ref} &= \tfrac{2}{3} \cdot \left(\tfrac{1}{E_d^2+E_q^2}\right) \cdot \left(E_q \cdot p_{ac}^{ref} - E_d \cdot q_{ac}^{ref}\right) \end{aligned} \tag{25}$$

where p_{ac}^{ref} and q_{ac}^{ref} are the references for the active and the reactive power respectively. it is necessary to have in count the active power that the system is delivering, in order to never exceed its limit. For this reason, the part on of p_{ac}^{ref} in (25) is redefined as:

$$\begin{aligned} x_1^{ref} &= \tfrac{2}{3} \cdot \left(\tfrac{1}{E_d^2+E_q^2}\right) \cdot \left(E_d \cdot \alpha \cdot p_{ac}^{ref} + E_q \cdot q_{ac}^{ref}\right) \\ x_2^{ref} &= \tfrac{2}{3} \cdot \left(\tfrac{1}{E_d^2+E_q^2}\right) \cdot \left(E_q \cdot \alpha \cdot p_{ac}^{ref} - E_d \cdot q_{ac}^{ref}\right) \end{aligned} \tag{26}$$

where α is calculated as given by:

$$\alpha = \begin{cases} 1 & if \quad z^{min} < z < z^{max} \\ 0 & if \quad otherwise \end{cases} \tag{27}$$

4 Test system and simulation scenarios

4.1 The studied system

Figure 3 shows the connection of the EESS to the power systems distribution, whose parameters are listed in Table 2. It is worth noting that both, the SMES and the SCES are able to store the same amount of energy.

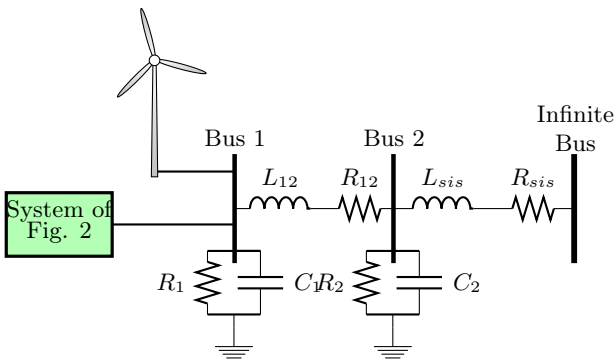

Figure 3: Radial distribution network with a renewable resources

4.2 Simulation scenarios

To demonstrate the robustness of the proposed control strategy the following scenarios are considered:

- First scenario: Verify the capability of the proposed controller to support (independently) active and reactive power considering the operating limits of the EESS.

Table 2: Parameters for Simulation

Parameter	Value	Unit	Parameter	Value	Unit
L_{sis}	2.5	mH	R_{sis}	5	$m\Omega$
L_{12}	1.5	mH	R_{12}	10	$m\Omega$
L_T	2.5	mH	R_T	1.25	$m\Omega$
L_{SC}	7.5	H	R_1	1	Ω
R_2	1	Ω	C_1	0.1	μF
C_2	0.1	μF	C_f	160	μF
C_{SC}	0.075	F	i_{dc}^{max}	100	A
i_{dc}^{min}	25	A	v_{dc}^{max}	1000	V
v_{dc}^{min}	250	V	v_{LL}^{rms}	440	V

- Second scenario: Evaluate the robustness of the proposed controller considering voltage unbalance and the introduction of harmonics in the infinite bus.
- Third scenario: Evaluate the accuracy of the proposed controller considering distributed energy resources.

For the first two scenarios, it is considered that the EESS is fully charged. For the third scenario it is considered that the EESS is charged up to 90%. Additionally, to evaluate the dynamical performance of the proposed LMI controller for the EESS, a comparison with the classical proportional integral controller is made.

5 Results

All suggested scenarios are carry-out in a time domain simulating software using Ordinary Differential Equations packages ODE23tb.

5.1 First scenario

In this part it is shown the ability of the proposed controller to regulate the active and reactive power in the EESS, which values are selected and listed in Table 3.

Table 3: Active and reactive power references values

Variable	Value $[kW]$ and $[kVAr]$	t_i [s]	t_f [s]
p_{ac}^{ref}	0	0	2
	3	2	6
	-2	6	10
	2	10	12
q_{ac}^{ref}	0	0	4
	-4	4	8
	4	8	10
	-2	10	12

Figure 4 shows the dynamical response at the dc side of the SMES, the active and reactive power variations, and the profile of the modulation indexes (m_d and m_q).

Figure 4a illustrates the behavior of the i_{dc} current which is directly influence by the active power being transference between the SMES and the ac grid, whereas the reactive power characteristic does not affect the current i_{dc}. This entails the possibility to provide reactive power by the power converter without the influence oh the SMES.

Notice that when p_{ac} is zero, the current i_{dc} remain constant because no power is transfered between the SMES and ac grid. When p_{ac} gets positive, the SMES provides energy to the ac grid. Because of that it is possible controller the energy storage of form indirect with active power control.

Figure 4b shows the active and reactive power in bus 1. The proposed controller responds appropriately with an average error of $5 \cdot 10^{-2}$ %. Also, a variation in the reference for both the p_{ac}^{ref} and q_{ac}^{ref} takes place at 10 s, as shown, the control action brings the power ans reactive power to the desired value. On the other hand, Figure 4c shows that the modulation indexes m_d and m_q do not reach saturation levels. Additionally, it is possible to observe that both are constants when p_{ac} is zero.

Figure 5 shows the dynamical responses at the dc side of the SCES, the active and reactive power variations, and the profile of the modulation indexes (m_d and m_q).

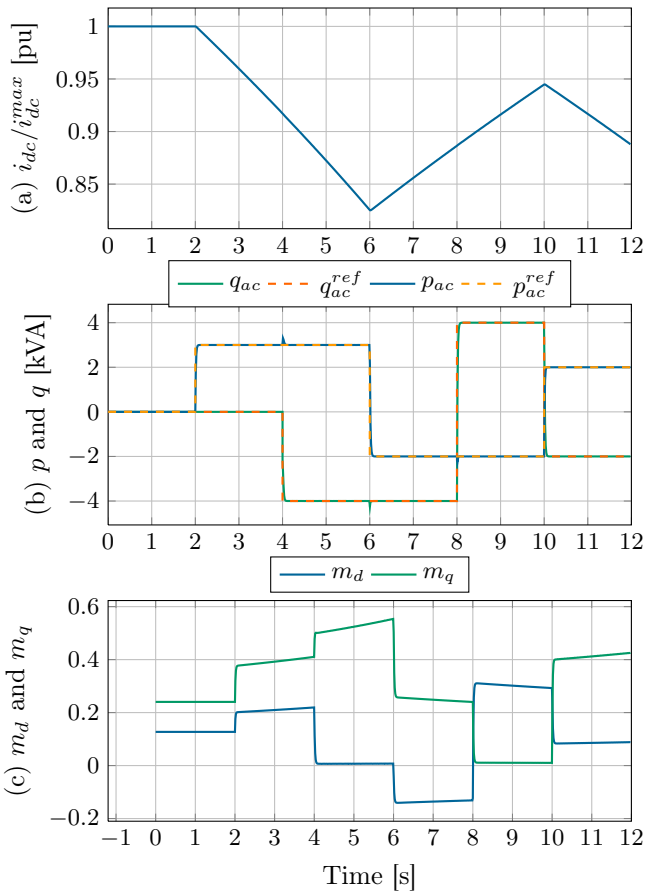

Figure 4: Dynamic response of the active and reactive power for the first scenario for SMES: (a) superconducting coil current i_{dc}, (b) active and reactive power delivered by the SMES system, and (c) modulation indexes m_d and m_q

In the case for the SCES the dynamical behavior of the voltage v_{dc} and the active power have the same behavior that the presented for the SMES (see Figures 5a and 5b). As indicated in Figures 4a and 5a, the profile of the energy for the SMES and the SCES is equal (represented for i_{dc} and v_{dc} respectively), because in the design of both EESS have of the same capacity. In this case, the average error is $6.5 \cdot 10^{-2}$ %. The modulation indexes also

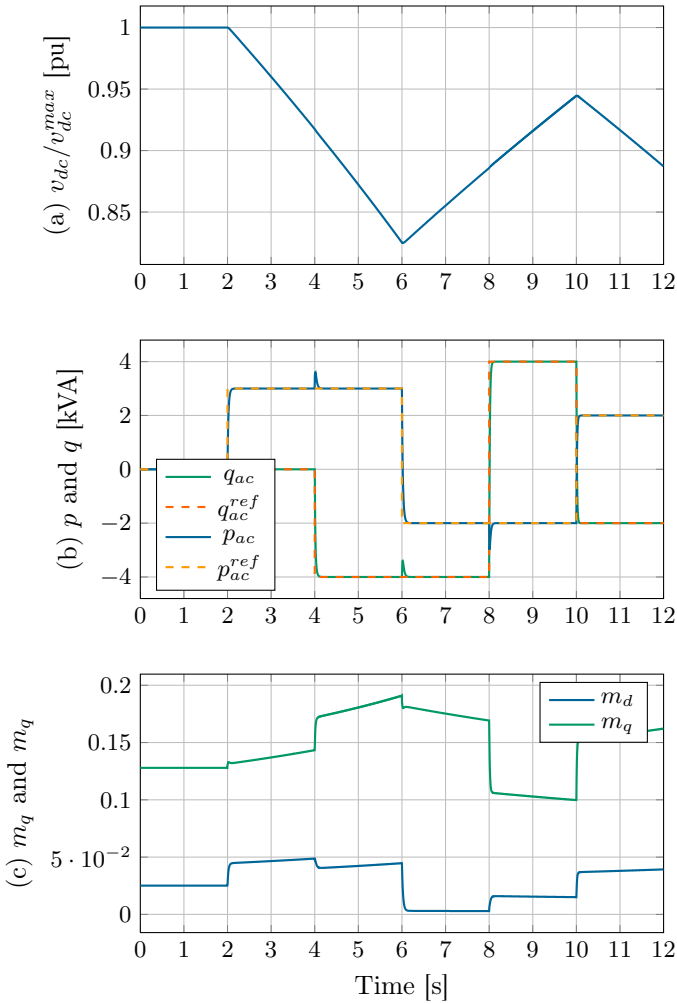

Figure 5: Dynamic response of the active and reactive power for the first scenario for SCES: (a) superconducting coil current i_{dc}, (b) active and reactive power delivered by the SCES system, and (c) modulation indexes m_d and m_q

present a similar approach to the modulations indexes for SMES as shown in Figure 4c (compare to 5c). The most notable difference between the modulation indexes is their magnitudes because the upper limits of energy

storage variables are very different (see Eqs. 6 and 10, and Table 2).

In this scenario is demonstrated the ability to independently control the active and reactive power by the proposed controller for both cases. Remark that, in this scenario there was not difference between the proposed control and PI controller, because of this the results were not shown for PI controller.

5.2 Second scenario

In this scenario, it is shown the robustness of the proposed control to active and reactive independently in the EESS. This objective considered two cases of operation on voltage of the Thevenin equivalent circuit of the grid (infinite bus). First, it is considered a voltage unbalance of about 5 % in each phase as follows: $|e_a(t)| = v_{LL}^{rms}$, $|v_b(t)| = 1.05 \cdot v_{LL}^{rms}$ and $|v_c(t)| = 0.95 \cdot v_{LL}^{rms}$. Second, it is considered high-magnitude harmonics for the a-phase, as follows:

$$v_a(t) = \sqrt{\frac{2}{3}} \cdot 440 \cdot \begin{bmatrix} \cos(\omega \cdot t) + \\ \frac{1}{5} \cdot \cos\left(5 \cdot \omega \cdot t - \frac{\pi}{6}\right) + \\ \frac{1}{10} \cdot \cos\left(7 \cdot \omega \cdot t - \frac{\pi}{3}\right) \end{bmatrix} V \tag{28}$$

The others phases contemplate the same high-magnitude harmonics considering positive sequence. Additionally, it is considered the same active and reactive power references used in the first scenario. In Figures 6 and 7 the response of the SMES and SCES in the ac equivalent bus 1 is illustrated.

Figures 6 and 7 show that the proposed control responds adequately under these operating conditions, although it has oscillations. This occurs because at every time instant the references change and the integral action of the proposed controller is not able to reach the desired value.

For the case of unbalanced voltages (see Figures 6a and 7a), the active power control of the SMES and SCES oscillates about ±1.32 % and ±3.53 % respectively, when the proposed controller is used. When PI controller is used the oscillations is about ±1.51 % for the SMES and ±3.72 % for the SCES. These oscillations occur between 4 s to 6 s for both EESS.

The reactive power control for the SMES and SCES oscillates about ±1.23 % and ±1.72 % respectively, when the proposed controller is used.

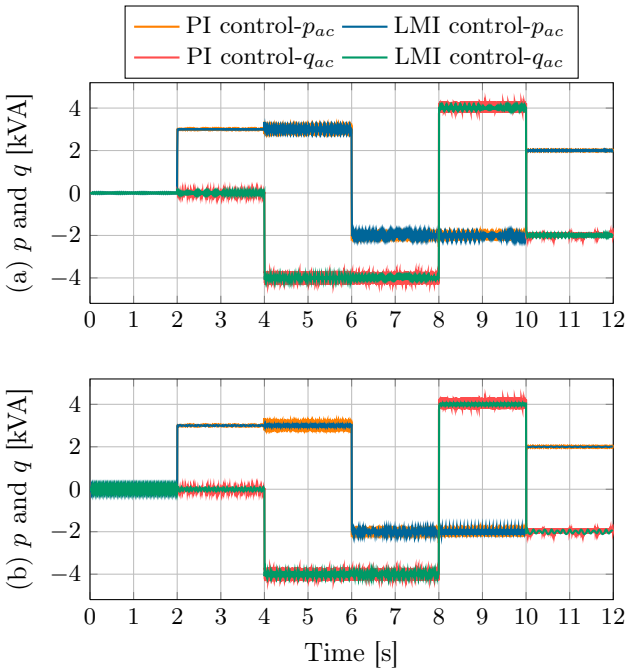

Figure 6: Dynamic response of the active and reactive power for the second scenario for SMES: (a) active and reactive power for unbalanced voltages, and (b) active and reactive power for high-magnitude harmonics content

When PI controller is used the oscillations is about ±1.31 % for SMES and ±2.51 % for SCES. These oscillations between 6 s to 8 s for the SMES and between 8 s to 10 s for the SCES.

For the case of high-magnitude harmonics distortion (see Figures 6b and 7b), the active power control of the SMES and SCES presents oscillations of about ±1.52 % and ±9.09 % respectively, when the proposed controller is used. When PI controller is used the oscillations is about ±2.16 % for the SMES and ±10.18 % for the SCES. These oscillations occur between 4 s to 6 s for both devices.

The reactive power control for the SMES and SCES shows oscillations of about ±1.52 % and ±1.44 % respectively, when the proposed controller is used. When PI controller is used the oscillations is about ±1.83 % for

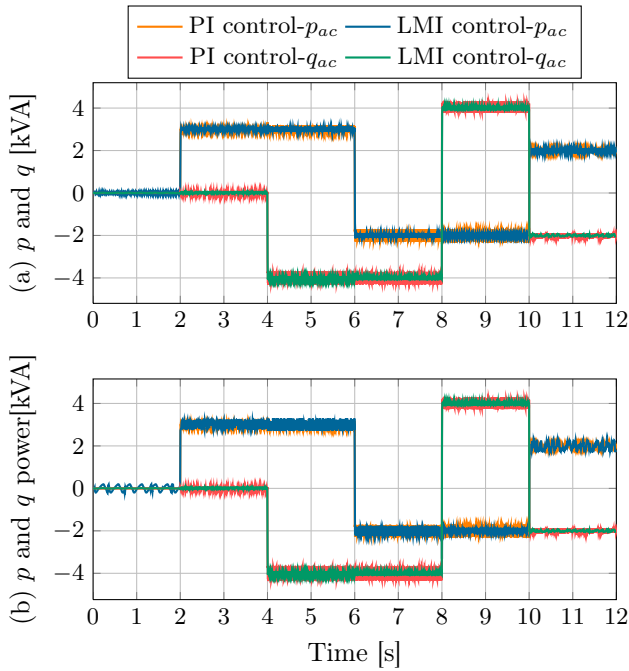

Figure 7: Dynamic response of the active and reactive power control for the second scenario for SCES: (a) active and reactive power for unbalanced voltages, and (b) active and reactive power for high-magnitude harmonics content

the SMES and ±2.17 % for the SCES. These oscillations occur between 4 s to 6 s for the SMES and between 8 s to 10 s for the SCES.

Notice that the active and reactive power control for both cases, are able to follow the references p^r_{ac} and q^r_{ac}, which show the robustness of LMI controllers to operate EESS in ac the grid.

In case of modulation indexes and energy storage variables analysis, these have a similar dynamical behavior as in the first simulation scenario; for this reason, their graphics are not presented.

5.3 Third scenario

In this scenario, it is presented the possibility to use the EESS to support active and reactive power in distributed generation applications. In this scenario, it is considered a wind turbine generator type 1 (Squirrel-cage Induction Generator-SCIG) connected in the bus-1 (see Figure 3) which inject active power and absorb reactive power. Recall that an SCIG turbine requires reactive power from the grid since the induction machine requires magnetization.

For the simulation implementation it is considered that the wind generator has been dispatched with an active power generation of 2500 W. However, the real power is variable and requires to be compensated by the EESS. Also, at the same time reactive power be kept in 0 $kVAr$. The parameters of the induction generator given in Table 4 was taking from [22].

Table 4: Parameters of the induction generator

V_{nom}^{rms}	$r_1[\Omega]$	$r_2[\Omega]$	$X_1[\Omega]$	$X_2[\Omega]$	$X_m[\Omega]$
440	0.641	0.332	1.106	0.464	78.9

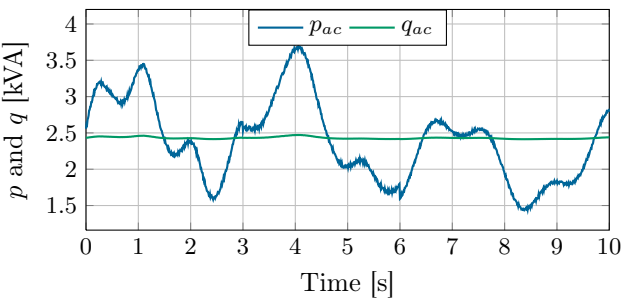

Figure 8: Active and reactive power of SCIG

The stored energy, active and reactive power output in the bus 1 for SMES are show in Figure 9 and in Figure 10 for SCES.

The dynamical response of energy stored in the EESS had the same behaviour as to be expected (see Figures 9a and 10a), since that reference

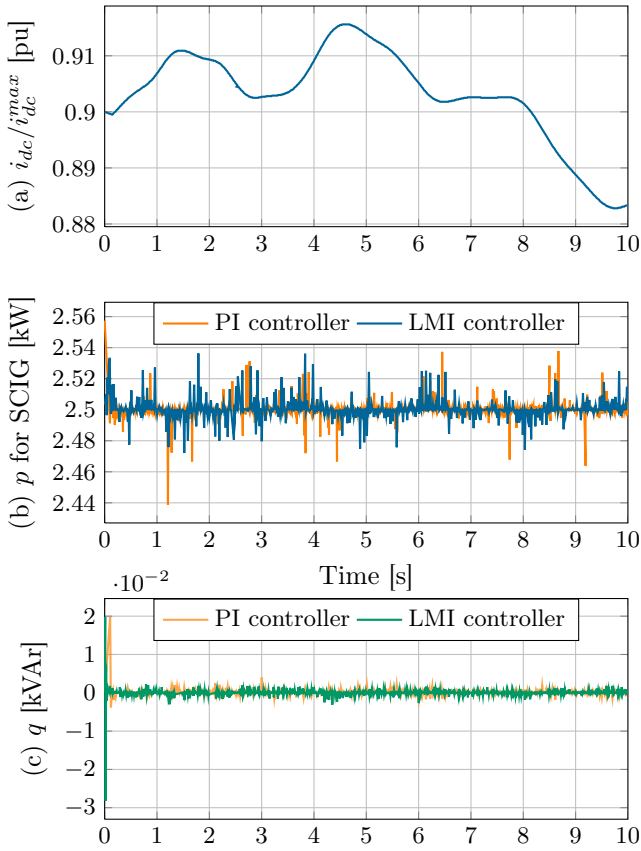

Figure 9: Dynamic response of the active and reactive power for the third scenario for SMES: (a) superconducting coil current and (b) active, and reactive power compensation using SMES

value of P_{ac}^{ref} was the same. To comparing active power of the Figure 8 with i_{dc} current of SMES of the 9a can be seen that i_{dc} current increased when the generated power by SCIG was greater than the dispatched power and it decreased otherwise. This also occurred in the case for SCES.

The Figures 9b and 10b shown the accuracy of the proposed control to keep the active power at 2500 W and it do not to generate a penalty in the grid operator. In this case, active power was a standard deviation of

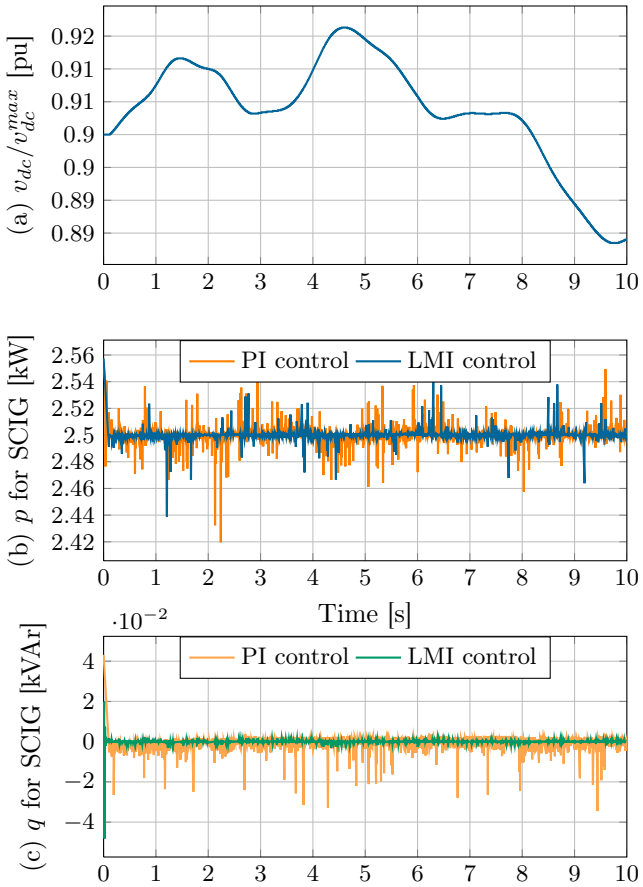

Figure 10: Dynamic response of the active and reactive power for the third scenario for SCES: (a) supercapacitor voltage, and (b) active and reactive power compensation using SCES

0.67 % and 0.74 % for SMES and SCES respectively (for PI controller were 0.79 % and 0.96 % for SMES and SCES respectively). Also, the reactive power was maintained at 0 $kVAr$ (see Figures 9b and 10b) thus improving the power factor in bus-1 by passing of an average power factor from 0.68 ↓ to 1.

6 Conclusions

In this paper a generalized mathematical linear model for EESS was presented. The model considers the dynamic of the power electronic interface used to connect the EESS (SMES or SCES) with the ac grid. An LMI-based state-feedback controller to obtain a general control law was selected because its capability to guarantee stability of the system in closed-loop. The proposed control strategy provided good performance to independently control active and reactive power of the EESS in a wide range of operating conditions even in the presence of unbalance voltage conditions and high-magnitude harmonic distortion at the ac grid side. As indicated in the third scenario, the proposed controller can be implemented to control the active power, reducing the power fluctuations in electric distribution systems with high penetration of renewable, such as wind power. The proposed controller showed good behavior helping the EESS to provide reactive power to keep unity power factor.

On the other hand, it is worth noting that the proposed controller has a better response when compared to conventional PI controller in all, which makes it an attractive control strategy to be applied in the support of active and reactive power. In addition, the proposed controller also has the advantage of not needing tuning. As a future work, the proposed controller will be implemented in microgrid system consisting of synchronous generator, wind generator, PV-system, constant loads and variable loads.

Acknowledgments

The authors want to thanks the support from the Administrative Department of Science, Technology and Innovation of Colombia (COLCIENCIAS), by calling contest 727-2015 and PhD program in Engineering at Universidad Tecnológica de Pereira.

References

[1] A. Ortega and F. Milano, "Generalized model of VSC-Based energy storage systems for transient stability analysis," *IEEE Trans. Power Syst.*, vol. 31, no. 5, pp. 3369–3380, Sept 2016. 148, 149

[2] J. Fang, W. Yao, Z. Chen, J. Wen, and S. Cheng, "Design of anti-windup compensator for energy storage-based damping controller to enhance power system stability," *IEEE Trans. Power Syst.*, vol. 29, no. 3, pp. 1175–1185, May 2014. 148

[3] A. Pappachen and A. P. Fathima, "Load frequency control in deregulated power system integrated with SMESâ"TCPS combination using ANFIS controller," *Int. J. Electr. Power Energy Syst.*, vol. 82, pp. 519 – 534, Nov. 2016. 148

[4] M. Farahani and S. Ganjefar, "Solving LFC problem in an interconnected power system using superconducting magnetic energy storage," *Physica C*, vol. 487, pp. 60 – 66, Apr. 2013. 148, 149

[5] M. Rabbani, J. Devotta, and S. Elangovan, "Multi-mode wide range subsynchronous resonance stabilization using superconducting magnetic energy storage unit," *International Journal of Electrical Power & Energy Systems*, vol. 21, no. 1, pp. 45 – 53, Jan. 1999. 149

[6] M. Farahani, "A new control strategy of SMES for mitigating subsynchronous oscillations," *Physica C*, vol. 483, pp. 34 – 39, Dec. 2012. 149

[7] M. Farhadi and O. Mohammed, "Energy storage technologies for high-power applications," *IEEE Trans. Ind. Appl.*, vol. 52, no. 3, pp. 1953–1961, May 2016. 149

[8] M. H. Ali, B. Wu, and R. A. Dougal, "An overview of SMES applications in power and energy systems," *IEEE Trans. Sustainable Energy*, vol. 1, no. 1, pp. 38–47, 2010. 149

[9] J. Shi, Y. Tang, K. Yang, L. Chen, L. Ren, J. Li, and S. Cheng, "SMES based dynamic voltage restorer for voltage fluctuations compensation," *IEEE Trans. Appl. Supercond.*, vol. 20, no. 3, pp. 1360–1364, 2010. 149

[10] E. Giraldo and A. Garces, "An adaptive control strategy for a wind energy conversion system based on pwm-csc and pmsg," *IEEE Trans. Power Systems*, vol. 29, no. 3, pp. 1446–1453, May 2014. 149

[11] A. Rahim and E. Nowicki, "Supercapacitor energy storage system for fault ride-through of a DFIG wind generation system," *Energy Convers. Manage.*, vol. 59, pp. 96 – 102, 2012. 149

[12] S. Wang and J. Jin, "Design and analysis of a fuzzy logic controlled smes system," *IEEE Trans. Appl. Supercond.*, vol. 24, no. 5, pp. 1–5, Oct 2014. 149

[13] M. H. Ali, M. Park, I. K. Yu, T. Murata, and J. Tamura, "Improvement of wind-generator stability by fuzzy-logic-controlled smes," *IEEE Trans. Ind. Appl.*, vol. 45, no. 3, pp. 1045–1051, May 2009. 149

[14] Jing Shi, Yuejin Tang, Li Ren, Jingdong Li, and Shijie Cheng, "Discretization-Based Decoupled State-Feedback Control for Current Source Power Conditioning System of SMES," *IEEE Trans. Power Delivery*, vol. 23, no. 4, pp. 2097–2104, Oct 2008. 149, 151

[15] J. Shi, L. Zhang, K. Gong, Y. Liu, A. Zhou, X. Zhou, Y. Tang, L. Ren, and J. Li, "Improved discretization-based decoupled feedback control for a series-connected converter of scc," *IEEE Trans. Appl. Supercond.*, vol. 26, no. 7, pp. 1–6, Oct 2016. 149, 152

[16] A. D. Giorgio, F. Liberati, A. Lanna, A. Pietrabissa, and F. D. Priscoli, "Model predictive control of energy storage systems for power tracking and shaving in distribution grids," *IEEE Trans. Sustainable Energy*, vol. 8, no. 2, pp. 496–504, April 2017. 149

[17] W. Gil-González, O. D. Montoya, A. Garcés, and A. Escobar-Mejía, "Supervisory LMI-based state-feedback control for current source power conditioning of SMES," in *2017 Ninth Annual IEEE Green Technologies Conference (GreenTech)*, March 2017, pp. 145–150. 149

[18] M. Grant and S. Boyd, "CVX: Matlab software for disciplined convex programming, version 2.1," Oct 2016. [Online]. Available: http://cvxr.com/cvx/ 150

[19] W. Gil-González, O. D. Montoya, A. Garcés, and G. Espinosa-Pérez, "IDA-passivity-based control for superconducting magnetic energy storage with PWM-CSC," in *2017 Ninth Annual IEEE Green Technologies Conference (GreenTech)*, March 2017, pp. 89–95. 151

[20] S. Boyd, L. El Ghaoui, E. Feron, and V. Balakrishnan, *Linear Matrix Inequalities in System and Control Theory*, ser. Studies in Applied Mathematics. Philadelphia: SIAM, Jun 1994, vol. 15, ch. 1. 153, 155

[21] E. Giraldo, *Multivariable Control*, 1st ed. Bergisch Gladbach: Scholar's Press, 2016, ch. 2. 155

[22] S. Chapman, *Electric Machinery Fundamentals*, ser. Electric machinery fundamentals. McGraw-Hill Companies, Incorporated, 2005. 166